EPJ Web of Conferences **191**, 02015 (2018) https://doi.org/10.1051/epjconf/201819102015
QUARKS-2018

Equivalent photons at the LHC: $pp(\gamma\gamma) \to pp\ell^+\ell^-$, $\mathrm{Pb\,Pb}\,(\gamma\gamma) \to \mathrm{Pb\,Pb}\,\ell^+\ell^-$

Mikhail Vysotsky[1,2,3,*] *Evgenii* Zhemchugov[1,3,**]

[1]Institute for Theoretical and Experimental Physics, 117218, Moscow, Russia
[2]National Research University Higher School of Economics, 101978, Moscow, Russia
[3]Moscow Engineering Physics Institute, 115409, Moscow, Russia

Abstract. The Large Hadron Collider is considered as a photon-photon collider with the photons produced in ultraperipheral collisions of protons or heavy ions. The equivalent photon approximation is applied to derive analytical formulae for the fiducial cross sections of reactions $pp(\gamma\gamma) \to pp\,\mu^+\mu^-$ and $\mathrm{Pb\,Pb}\,(\gamma\gamma) \to \mathrm{Pb\,Pb}\,\mu^+\mu^-$. The results are compared to the measurements reported by the ATLAS collaboration.

1 Introduction

The Large Hadron Collider was conceived as a quark/gluon collider (hence the name), yet it can also act as a photon-photon collider with the photons produced in ultraperipheral collisions. A peripheral collision occurs when the impact parameter of the collision is larger than the sum of the radii of particles. An ultraperipheral collision is a peripheral collision with one or both of the colliding particles surviving the collision. In this paper only the collisions with both of the colliding particles remaining intact after the collision will be considered.

Ultraperipheral collisions make a considerable fraction of collisions at the LHC. They provide an opportunity to study electroweak processes at high energies. Cross section of a collision mediated by photons is proportional to Z^4 where Ze is the charge of the colliding particles. It makes heavy ions collisions look a lot more attractive when compared to protons as a source of photons at the LHC. Let us compare the data collected in Run 2 in proton-proton collisions and in the heavy ions run which took place in 2015:

- Integrated luminosity provided by the LHC to the CMS in Run 2: 111 fb^{-1} as of May 27, 2018 [1]; expected at the end of Run 2 in 2018: 150 fb^{-1}.
- Integrated luminosity provided by the LHC to the CMS in the heavy ions run in 2015: 0.6 nb^{-1} [1].
- Luminosity ratio (expected): $2.1 \cdot 10^8$.
- For Pb, $Z = 82$; $Z^4 \approx 4.5 \cdot 10^7$.

Taking ratio of these numbers, we get that if there exists New Physics that could appear in photon-photon collisions, there will be about 5 times more events of it in pp collisions at the end of Run 2 than there were in Pb Pb collisions in 2015. However, the heavy ions run

*e-mail: vysotsky@itep.ru
**e-mail: zhemchugov@itep.ru

© The Authors, published by EDP Sciences. This is an open access article distributed under the terms of the Creative Commons Attribution License 4.0 (http://creativecommons.org/licenses/by/4.0/).

duration was about 20 days, while Run 2 is scheduled to take ≈ 500 days not counting the 2015 when only 4.2 fb^{-1} were collected. Hence, one can raise a question on whether the LHC schedule should provide more time for the heavy ions collisions so that New Physics can be searched in photon-photon collisions. This question might be most relevant now, with the long shutdown of the LHC beginning this winter, so that the necessary detector adjustments could be made, and the future LHC schedule could be negotiated.

The estimation presented above is very rough. To consider possible advantages of ultra-peripheral collisions in a more rigid way, concrete models of New Physics should be selected and experimental signatures should be calculated. The signatures can be obtained through the equivalent photon approximation. In [2], the equivalent photon approximation is used to obtain analytical formulae for the fiducial cross sections of muon pair production in ultra-peripheral collisions of protons or lead nuclei. The main results of this paper are presented here. In the future, these results ought to be useful in discussing possible production of New Physics particles.

2 Equivalent photon approximation

In the equivalent photon approximation (EPA) [3–6] (see also [7–9]), the electromagnetic field of an ultrarelativistic charged particle is replaced with a set of photons distributed according to the function

$$n(\vec{q})\,\mathrm{d}^3q = \frac{Z^2\alpha}{\pi^2}\frac{\vec{q}_\perp^{\,2}}{\omega q^4}\mathrm{d}^3q, \tag{1}$$

where q is the photon 4-momentum, $\vec{q}_\perp$ is it transverse component, and ω is the photon energy. The photons are almost real, with their virtuality

$$-q^2 = (\omega/\gamma)^2 + \vec{q}_\perp^{\,2} \ll \omega^2, \tag{2}$$

where γ is the Lorentz factor of the particle. To obtain the spectrum of the equivalent photon approximation, $n(\omega)$, (1) should be integrated over $\mathrm{d}^2q_\perp$. The integral is divergent at large $|\vec{q}_\perp|$. Assuming a cutoff at some value $\hat{q}$, the equivalent photon spectrum in the limit $\omega \ll \hat{q}\gamma$ is

$$n(\omega)\,\mathrm{d}\omega = \frac{2Z^2\alpha}{\pi}\ln\left(\frac{\hat{q}\gamma}{\omega}\right)\frac{\mathrm{d}\omega}{\omega}. \tag{3}$$

In the case of a proton, the physical meaning of the spectrum cutoff value $\hat{q}$ is that when a proton emits a photon with momentum higher than $\hat{q}$, it breaks apart. Thus, $\hat{q}$ should be of the order of the inverse of the proton radius or the QCD scale $\Lambda_{\mathrm{QCD}} \approx 0.2$–$0.3$ GeV [10, Section 9]. A better estimation for the value of $\hat{q}$ can be obtained through consideration of proton electromagnetic form factors. Since $-q^2 \sim \hat{q}^2 \sim \Lambda_{\mathrm{QCD}}^2 \ll 4m_p^2$, only the electric form factor $G_E(q^2)$ is relevant in this process, where

$$G_E(q^2) = \left(1 - \frac{q^2}{\Lambda^2}\right)^{-2}, \tag{4}$$

$\Lambda^2 = 0.71$ GeV^2 [11]. Integration of the equivalent photon distribution with the form factor taken into account, $n'(\vec{q}) = n(\vec{q}) \cdot G_E(q^2)$, over the transverse momentum up to infinity results in

$$n'(\omega)\,\mathrm{d}\omega = \frac{2Z^2\alpha}{\pi}\left(\ln\frac{\Lambda\gamma}{\omega} - \frac{17}{12}\right)\frac{\mathrm{d}\omega}{\omega} \tag{5}$$

in the limit $\omega \ll \Lambda\gamma$. Comparison of (3) and (5) results in

$$\hat{q} = \Lambda e^{-\frac{17}{12}} \approx 204\ \text{MeV}, \tag{6}$$

which is in a perfect agreement with the assumption that $\hat{q} \sim \Lambda_{\text{QCD}}$.

In the case of a lead nucleus, a simplified form-factor of the same form as for the proton can be used with the parameter $\Lambda = 80$ MeV [12]. Then $\hat{q} \approx 20$ MeV.

3 Muon pair production

The leading order Feynman diagrams for the $pp(\gamma\gamma) \to pp\mu^+\mu^-$ reaction are presented in Fig. 1. The corresponding cross section is

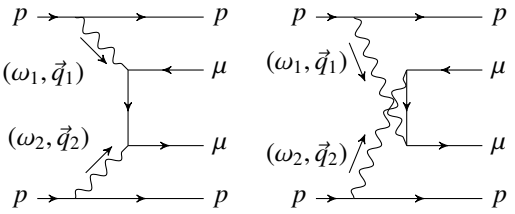

Figure 1. Leading order Feynman diagrams for the $pp(\gamma\gamma) \to pp\mu^+\mu^-$ reaction.

$$\sigma(pp(\gamma\gamma) \to pp\mu^+\mu^-) = \int\limits_{m_\mu^2/\hat{q}\gamma}^{\hat{q}\gamma} \mathrm{d}\omega_1 \int\limits_{m_\mu^2/\omega_1}^{\hat{q}\gamma} \mathrm{d}\omega_2\, \sigma(\gamma\gamma \to \mu^+\mu^-)\, n(\omega_1)\, n(\omega_2), \tag{7}$$

where $\sigma(\gamma\gamma \to \mu^+\mu^-)$ is the Breit-Wheeler cross section of lepton pair production in photon-photon collision [13].

It is convenient to change the integration variables to $s = 4\omega_1\omega_2$, $x = \omega_1/\omega_2$, with $\sqrt{s}$ being the invariant mass of the muons. Then

$$\sigma(pp(\gamma\gamma) \to pp\mu^+\mu^-) = \frac{\alpha^2}{2\pi^2} \int\limits_{(2m_\mu)^2}^{(2\hat{q}\gamma)^2} \frac{\mathrm{d}s}{s} \sigma(\gamma\gamma \to \mu^+\mu^-) \int\limits_{s/(2\hat{q}\gamma)^2}^{(2\hat{q}\gamma)^2/s} \frac{\mathrm{d}x}{x} \ln\frac{(2\hat{q}\gamma)^2}{sx} \ln\left[\frac{(2\hat{q}\gamma)^2}{s} \cdot x\right] \tag{8}$$

(note the symmetry of the integral under the $x \to 1/x$ replacement). After the integration, the final result is

$$\sigma(pp(\gamma\gamma) \to pp\mu^+\mu^-) = 8 \cdot \frac{28}{27} \frac{\alpha^4}{\pi m_\mu^2} \ln^3 \frac{\hat{q}\gamma}{m_\mu}. \tag{9}$$

This expression should be compared with Eq. (37) in [6]. The extra factor of 8 in (9) is because of different systems of reference: (9) is obtained in the center of mass of protons, while in [6] one of the colliding particles is at rest, hence the difference in γ. Also, [6] is considering electrons, and in this case $\hat{q}$ should be set equal to m_e, see [9].

The experimentally observed quantity is the fiducial cross section which is the regular cross section after applying experimental cuts on the phase space. The ATLAS collaboration has used the same kinds of cuts when measuring the muon pair production in proton-proton [14] and lead-lead [15] collisions:

- The cut on the invariant mass of muon pair $\sqrt{s}$, $\hat{s}_{\min} < s < \hat{s}_{\max}$, is used to suppress the background from vector meson decays into $\mu^+\mu^-$. This cut is trivial to apply—one just have to change the integration limits in the integration over s in (8) accordingly. A simplified expression for the Breit-Wheeler cross section can be used when $\sqrt{\hat{s}_{\min}} \gg m_\mu$:

$$\sigma(\gamma\gamma \to \mu^+\mu^-) \approx \frac{4\pi\alpha^2}{s}\left(\ln\frac{s}{m_\mu^2} - 1\right), \tag{10}$$

so

$$\sigma^{(\hat{s})}_{\text{fid.}}(pp(\gamma\gamma) \to pp\mu^+\mu^-) = \frac{64\alpha^4}{3\pi}\int\limits_{\hat{s}_{\min}}^{\hat{s}_{\max}}\frac{\mathrm{d}s}{s^2}\left(\ln\frac{s}{m_\mu^2} - 1\right)\ln^3\frac{2\hat{q}\gamma}{\sqrt{s}}. \tag{11}$$

- The cut on muon transverse momentum p_T, $p_T > \hat{p}_T$, is used to suppress the background from hadronic processes. This cut is taken into account by replacing the Breit-Wheeler cross section in (8) with the integral up to $\hat{p}_T$ of its differential with respect to p_T. Assuming $\sqrt{s_{\min}} \gg m_\mu$,

$$\frac{\mathrm{d}\sigma(\gamma\gamma \to \mu^+\mu^-)}{\mathrm{d}p_T} = \frac{8\pi\alpha^2}{sp_T}\frac{1 - 2p_T^2/s}{\sqrt{1 - 4p_T^2/s}}, \tag{12}$$

and

$$\sigma^{(\hat{s},\hat{p}_T)}_{\text{fid.}}(pp(\gamma\gamma) \to pp\mu^+\mu^-) = \frac{64\alpha^4}{3\pi}\int\limits_{\hat{s}_{\min}}^{\hat{s}_{\max}}\frac{\mathrm{d}s}{s^2}\ln^3\frac{2\hat{q}\gamma}{\sqrt{s}}\left(\ln\frac{1 + \sqrt{1 - 4\hat{p}_T^2/s}}{1 - \sqrt{1 - 4\hat{p}_T^2/s}} - \sqrt{1 - \frac{4\hat{p}_T^2}{s}}\right). \tag{13}$$

- The cut on muon pseudorapidity η, $|\eta| < \hat{\eta} = 2.4$, accounts for the detector geometry: muons with higher pseudorapidity evade the muon spectrometer. Pseudorapidity is defined as $\eta = -\ln\tan(\theta/2)$, where θ is the angle between the momentum of the muon and the beam axis, so $|\eta| < 2.4$ is equivalent to $10^\circ < \theta < 170^\circ$. For fixed s and p_T, the cut on η can be transformed to a cut on x, so the fiducial cross section

$$\sigma^{(\hat{s},\hat{p}_T,\hat{\eta})}_{\text{fid.}}(pp(\gamma\gamma) \to pp\mu^+\mu^-) = \frac{4\alpha^4}{\pi}\int\limits_{\hat{s}_{\min}}^{\hat{s}_{\max}}\frac{\mathrm{d}s}{s^2}\int\limits_{\hat{p}_T}^{\sqrt{s}/2}\frac{\mathrm{d}p_T}{p_T}\frac{1 - 2p_T^2/s}{\sqrt{1 - 4p_T^2/s}}\int\limits_{1/\hat{x}}^{\hat{x}}\frac{\mathrm{d}x}{x}\ln\frac{(2\hat{q}\gamma)^2}{sx}\ln\left(\frac{(2\hat{q}\gamma)^2}{s}\cdot x\right), \tag{14}$$

where

$$\hat{x} = \mathrm{e}^{2\hat{\eta}}\frac{1 - \sqrt{1 - 4p_T^2/s}}{1 + \sqrt{1 - 4p_T^2/s}}. \tag{15}$$

4 Comparison with the experimental data

4.1 $pp(\gamma\gamma) \to pp\mu^+\mu^-$

In [14], the fiducial cross section for the muon pair production in proton-proton collisions with the collision energy 13 TeV was measured to be

$$\sigma_{\text{fid.}}(pp(\gamma\gamma) \to pp\mu^+\mu^-) = 3.12 \pm 0.07\ (\text{stat.}) \pm 0.10\ (\text{syst.})\ \text{pb}. \tag{16}$$

The experimental cuts are:

Table 1. Fiducial cross sections for the reaction $pp(\gamma\gamma) \to pp\mu^+\mu^-$.

No cuts		$2.2 \cdot 10^5$ pb
12 GeV $< \sqrt{s} <$ 30 GeV	54.0 pb	59.6 pb
30 GeV $< \sqrt{s} <$ 70 GeV	5.65 pb	
12 GeV $< \sqrt{s} <$ 30 GeV, $p_T >$ 6 GeV	5.37 pb	6.28 pb
30 GeV $< \sqrt{s} <$ 70 GeV, $p_T >$ 10 GeV	0.91 pb	
12 GeV $< \sqrt{s} <$ 30 GeV, $p_T >$ 6 GeV, $\lvert\eta\rvert <$ 2.4	2.85 pb	3.35 pb
30 GeV $< \sqrt{s} <$ 70 GeV, $p_T >$ 10 GeV, $\lvert\eta\rvert <$ 2.4	0.50 pb	

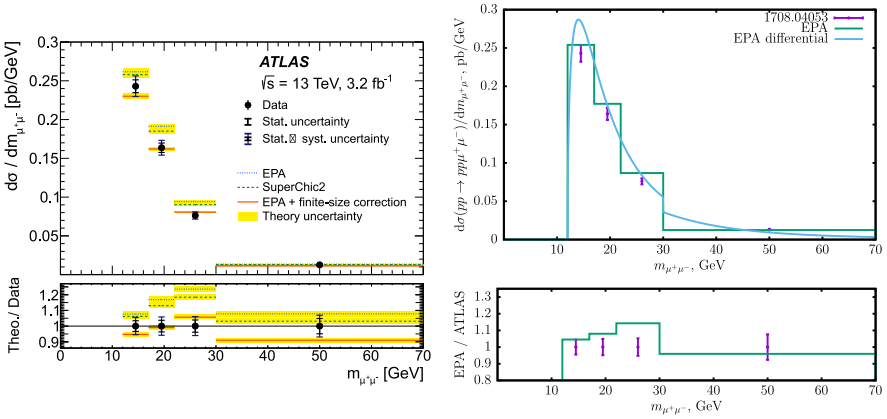

Figure 2. *Left plot:* Differential cross section for the muon pair production in proton-proton collision measured by the ATLAS collaboration. $m_{\mu\mu'} \equiv \sqrt{s}$ is the invariant mass of the muon system. Yellow bands correspond to the equivalent photon approximation with the fiducial cross section calculated with the help of Monte Carlo methods [16, 17]. This plot is taken from the ATLAS paper [14], Fig. 5a. *Right plot:* The points are copied from the left plot. The curve is the differential cross section calculated with the help of (14). The histogram is the differential cross section integrated over the same bins as the experimental points.

- for 12 GeV $< \sqrt{s} <$ 30 GeV: $p_T >$ 6 GeV, $|\eta| <$ 2.4;
- for 30 GeV $< \sqrt{s} <$ 70 GeV: $p_T >$ 10 GeV, $|\eta| <$ 2.4.

Results of successive application of cuts calculated with the help of (9), (11), (13), (14) are presented in Table 1. The differential cross section is presented in Fig. 2. The fiducial cross section calculated with the help of (14) is

$$\sigma_{\text{fid.}}^{(\hat{s},\hat{p}_T,\hat{\eta})}(pp(\gamma\gamma) \to pp\mu^+\mu^-) = 3.35 \text{ pb}, \tag{17}$$

and it is in agreement with the experimental result (16).

4.2 $\text{Pb}\,\text{Pb}\,(\gamma\gamma) \to \text{Pb}\,\text{Pb}\,\mu^+\mu^-$

In [15], the fiducial cross section for the muon pair production in lead-lead collisions with the collision energy per nucleon pair equal to 5.03 TeV was measured to be

$$\sigma_{\text{fid.}}(\text{Pb}\,\text{Pb}\,(\gamma\gamma) \to \text{Pb}\,\text{Pb}\,\mu^+\mu^-) = 32.2 \pm 0.3\,(\text{stat.})^{+4.0}_{-3.4}\,(\text{syst.})\,\mu\text{b}. \tag{18}$$

The experimental cuts are: 10 GeV $< \sqrt{s} <$ 100 GeV, $p_T >$ 4 GeV, $|\eta| <$ 2.4. Results of successive application of cuts are presented in Table 2. The differential cross section is

Table 2. Fiducial cross sections for the reaction $\mathrm{Pb\,Pb}\,(\gamma\gamma) \to \mathrm{Pb\,Pb}\,\mu^+\mu^-$.

No cuts	$2.80 \cdot 10^6$ μb
10 GeV $< \sqrt{s} <$ 100 GeV	119 μb
also $p_T > 4$ GeV	34.2 μb
also $\lvert\eta\rvert < 2.4$	30.9 μb

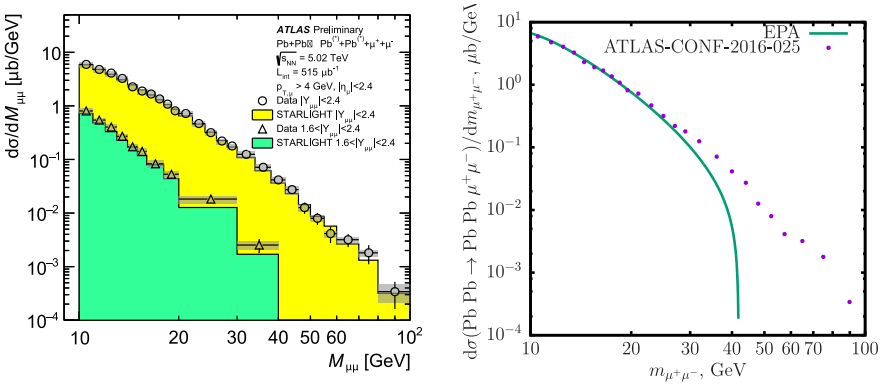

Figure 3. *Left plot:* Differential cross section for the muon pair production in lead-lead collision measured by the ATLAS collaboration. The two sets of data points correspond to two cuts on muon pair rapidity. The cut for the upper curve is equivalent to the cut on each muon pseudorapidity $|\eta| < 2.4$. The plot is taken from the ATLAS paper [15], Fig. 3. *Right plot:* The points are copied from the upper curve of the left plot. The line is the differential cross section calculated with the help of (14).

presented in Fig. 3. In the region of higher invariant masses the assumption $\omega \ll \hat{q}\gamma$ used in the derivation of the equivalent photon spectrum (3) is violated, and the cross section is cut off too early. Nevertheless, the major contribution to the integrated cross section is from the photons of lower energies, so the integrated fiducial cross section

$$\sigma_{\mathrm{fid.}}^{(\hat{s},\hat{p}_T,\hat{\eta})}(\mathrm{Pb\,Pb}\,(\gamma\gamma) \to \mathrm{Pb\,Pb}\,\mu^+\mu^-) = 30.9\ \mu\mathrm{b} \tag{19}$$

was found to be in agreement with the experimental result (18).

5 Conclusions

The LHC can be used to search for New Physics in photon-photon collisions with the photons produced in ultraperipheral collisions of protons or heavy ions. Photon invariant mass can reach $2\hat{q}\gamma \approx 2.8$ TeV in pp collisions with the collision energy equal to 13 TeV, and $\approx$ 100 GeV in Pb Pb collisions with the collision energy per nucleon pair equal to 5.03 TeV.

Analytical formulae for the fiducial cross section of lepton pair production in ultraperipheral collisions of charged particles were derived. Fiducial cross sections calculated for the reactions $pp(\gamma\gamma) \to pp\mu^+\mu^-$ and $\mathrm{Pb\,Pb}\,(\gamma\gamma) \to \mathrm{Pb\,Pb}\,\mu^+\mu^-$ were found to be in agreement with the experimental data.

We are grateful to the organizers for an inspiring conference held in a beautiful place. We were supported by the RFBR grant 16-02-00342.

References

[1] CMS Luminosity—Public Results
https://twiki.cern.ch/twiki/bin/view/CMSPublic/LumiPublicResults

[2] M. I. Vysotsky, E. V. Zhemchugov. Equivalent photons in photon-photon and ion-ion collisions at the LHC. arXiv:1806.07238 (2018).

[3] E. Fermi. Über die Theorie das Stoßes zwischen Atomen und elektrisch geladenen Teilchen. Z.Physik 29, 315 (1924).

[4] C. F. V. Weizsäcker. Ausstrahlung bei Stößen sehr schneller Elektronen. Z.Physik 88, 612 (1934).

[5] E. J. Williams. Correlation of certain collision problems with radiation theory. Kgl. Danske Vidensk. Selskab. Mat.-Fiz. Medd. 13, 4 (1935).

[6] L. D. Landau, E. M. Lifshitz. Production of electrons and positrons by a collision of two particles. Phys.Zs.Sowjet 6, 244 (1934).

[7] H. Terazawa, Two-photon processes for particle production at high energies. Rev.Mod.Phys. 4, 615 (1973).

[8] V. M. Budnev, I. F. Ginzburg, G. V. Meledin, V. G. Serbo. The two-photon particle production and the equivalent photon approximation. Particles & Nuclei 4, 239 (1973) [in Russian].

[9] V. M. Budnev, I. F. Ginzburg, G. V. Meledin, V. G. Serbo. The two-photon particle production mechanism. Physical problems. Applications. Equivalent photon approximation. Phys.Rep. 15, 181 (1975)

[10] Particle Data Group. Review of Particle Physics. Chinese Physics C 40, 100001 (2016).

[11] S. Pacetti, R. B. Ferroli, E. Tomasi-Gustafsson. Proton electromagnetic form factors: basic notions, present achievements and future perspectives. Phys.Rep. 550, 1 (2015).

[12] U. D. Jentschura, V. G. Serbo. Nuclear form factor, validity of the equivalent photon approximation and Coulomb corrections to muon pair production in photon-nucleus and nucleus-nucleus collisions. Eur.Phys.J. C64, 309 (2009). arXiv:0908.3853

[13] G. Breit, J. A. Wheeler. Collision of two light quanta. Phys.Rev. 46, 1087 (1934).

[14] The ATLAS Collaboration. Measurement of the exclusive $\gamma\gamma \to \mu^+\mu^-$ process in proton-proton collisions at $\sqrt{s} = 13$ TeV with the ATLAS detector. Phys.Lett. B 777, 303 (2018). arXiv:1708.04053

[15] The ATLAS Collaboration. Measurement of high-mass dimuon pairs in ultra-peripheral lead-lead collisions at $\sqrt{s_{NN}} = 5.02$ TeV with the ATLAS detector at the LHC. ATLAS-CONF-2016-025 (2016).

[16] L. A. Harland-Lang, V. A. Khoze, M. G. Ryskin. Exclusive physics at the LHC with SuperChic 2. Eur.Phys.J. C76, 9 (2016). arXiv:1508.02718

[17] M. Dyndal, L. Schoeffel. The role of finite-size effects on the spectrum of equivalent photons in proton-proton collisions at the LHC. Phys.Lett.B 741, 66 (2015). arXiv: 1410.2983